

SPIN-LATTICE RELAXATION IN THE TRIPLET STATE OF THE BURIED TRYPTOPHAN RESIDUE OF RIBONUCLEASE T₁

SANJIB GHOSH, MICHAEL PETRIN, AND AUGUST MAKI

Department of Chemistry, University of California Davis, California, 95616

ABSTRACT The individual spin-lattice relaxation (SLR) rate constants (W_{ij}) between the lowest triplet sublevels of the lone tryptophan residue buried in the interior of the globular protein ribonuclease T₁ have been reported in the temperature range 1.2 to 3.0 K in zero applied magnetic field. The SLR rate constants between spin sublevels exhibit marked anisotropy in their magnitudes and also show appreciable sensitivity to the glycerol content of the aqueous cryogenic matrix. The temperature dependence of SLR suggests that in the temperature range investigated a direct process contributes dominantly to the SLR in this protein.

INTRODUCTION

Although there have been reports of spin-lattice relaxation (SLR) rate constants in the triplet state of emitting tryptophan residues in several proteins in zero magnetic field at 1.2 K, mechanisms involved in these relaxation processes have not been addressed (1–3). This type of investigation seems necessary in order to explore any correlation between SLR rates and the subtle structural variability in the vicinity of tryptophan residues in proteins, which is not readily accessible by other conventional methods. Recently, correlation between protein structure and the temperature dependence of the electron spin relaxation rate has been shown to exist in paramagnetic iron proteins (4, 5). In these investigations, a Raman relaxation rate was found exhibiting a $T^{(3+2d)}$ temperature dependence, where d represents the fractal dimension of the entire biopolymer (5).

In the case of the triplet state of organic molecules, several possible SLR mechanisms have been suggested, including; (a) spin-orbit-lattice phonon coupling, which acts via spin-orbit interactions on the T₁ state; (b) modulation of electron dipole-dipole coupling by phonons; and (c) the modulation of hyperfine interactions by phonons. The work of Wolfe (6) and of Fischer and Dennison (7) in high field suggests that mechanism (b) is largely responsible for SLR in the triplet states of organic molecules. Verbeek et al. (8) have concluded that the SLR rate in the fast relaxation limit (e.g. where $W_{ij} \gg k_i$, $i = x, y, z$ and k is the total sublevel decay constant) for the case of naphthalene in durene arises from an Orbach type process (9) with an activation energy of ~ 16 cm⁻¹ (8). It was proposed that relaxation results from thermal excitation to a nearby local

phonon state, where the spin axes are rotated with respect to those in the lowest triplet state (8). These investigations predicted that since the rotation of spin axes occurs largely about the axis normal to the molecular plane, the dominant relaxation route should be between the in-plane zero field sublevels. Similar conclusions have been presented in the case of aniline in *p*-xylene (10) and zinc porphyrin (ZnP) in *n*-alkane matrices (11). Recently, however, SLR rates in the triplet state of naphthalene in an *n*-pentane Shpol'skii matrix, in the temperature range where the W_{ij} 's are either smaller or of a magnitude comparable to the k_i (slow or intermediate relaxation limit, respectively) were found to show different anisotropies (12). It was observed that the SLR rate between the two sublevels having the largest energy separation is dominant; the mechanism involved corresponded to a combination of direct and either Raman or Orbach relaxation processes.

In this paper the temperature dependence of individual SLR rate constants between the triplet sublevels of a tryptophan residue within a protein structure in zero magnetic field is reported for the first time. The globular protein ribonuclease T₁ from *Aspergillus oryzae* (RNase T₁) has been selected since it possesses only a single tryptophan residue, and because the well resolved phosphorescence emission spectrum and narrow zero field ODMR (optically detected magnetic resonance) line widths indicate a higher degree of homogeneity in the vicinity of the tryptophan residue than is typically observed in proteins (13). The method employed to extract SLR rate constants involves analysis and deconvolution of the phosphorescence decays during continuous microwave saturation of triplet sublevel populations in pairs. Microwave saturation produces a pseudo-two-level system which decays as the sum of two exponential components whose values can be expressed solely in terms of the individual k_i 's and W_{ij} 's

Correspondence should be addressed to Sanjib Ghosh.

(1, 14). This method allows one to determine the individual W 's when they are comparable to the k 's in magnitude, and does not require knowledge of the relative radiative rate constants. This study has also shown that changes in the solvent environment due to adjustment of the glycerol to aqueous phosphate buffer ratio of the medium produce measured effects on SLR rate constants in the triplet state of the lone tryptophan of RNase T₁. The measurements also provide a set of accurate total decay constants for the individual triplet sublevels of the tryptophan residue in this protein, which are compared to those obtained in other systems. Knowledge of accurate sublevel decay constants is important in consideration of energy transfer rates in proteins.

MATERIALS AND METHODS

Sample Preparation

Ribonuclease T₁ from *Aspergillus oryzae* was obtained from Sigma Chemical Company (St. Louis, MO). The ammonium sulfate suspension of RNase T₁ was dialyzed against 0.1 M phosphate buffer at pH 7.5 and concentrated. Different solutions composed of various ratios of glycerol (Gold Label, Aldrich Chemical Company, Milwaukee, WI) and phosphate buffer, and having a fixed enzyme concentration of $\sim 1.5 \times 10^{-4}$ M, were then prepared. Absorption and emission spectra confirmed the absence of any impurity emission in the sample or solvents.

Instrumental

Samples were pipetted into Suprasil tubes and placed within a tightly fitted microwave slow wave helix terminating a coaxial transmission line. This was then suspended in a dewar (Model 8DT, Janis Research Co, Wilmington, MA) that could be maintained at 4.2 K or below by pumping on the liquid helium. Samples were cooled slowly by inserting the helix in the dewar before transferring liquid helium. The temperature was maintained within ± 0.02 K by use of a pressure regulator valve (Model 329, Lake Shore Cryotronics, Westerville, OH) that provided temperature control over the pumped helium range of 1.2 to 4.2 K. The liquid helium bath temperature was monitored near the sample with a

calibrated germanium resistance diode (Lake Shore Cryotronics model GR-200A-250) accurate to within ± 0.01 K.

The excitation source was a 100 W high pressure mercury arc lamp and housing (Model ALH-215, Photochemical Research Associates, London, Ontario, Canada) followed by a 12 cm NiSO₄ (500 gm/liter) infrared solution filter and a 10 cm monochromator (Model H-10, Instruments SA, Metuchen, NJ). For decay measurements, the sample was excited at 305 nm with 8 nm slits to prevent tyrosine excitation. Emission at a right angle to the excitation path passed through a high pass WG-345-2 glass filter and was collected by a 1 m monochromator (Model 2051, GCA/McPherson Instrument Corp, Acton, MA) equipped with a 600 groove/mm grating and detected by a cooled photomultiplier tube (Model 9789 QA, Electron Measurements Inc, Neptune, NJ). Data analysis was performed on a Digital PRO-350 microcomputer (Digital Equipment Corp., Mainard, MA) interfaced to a 1024 channel signal averager (Model 1072, Nicolet Instrument Corp., Madison, WI), which collected all raw decay and phosphorescence data.

All ODMR measurements were performed while monitoring the 0,0-band emission maximum of tryptophan in RNase T₁ at 404.5 nm with a slit resolution of 0.75 nm. Microwave saturated phosphorescence decay (MSPD) measurements were performed in a manner described previously (1, 14). Sample excitation time was 30 s and the decay profile was followed for 30 s. Microwave saturation was achieved by frequency modulating at 2 kHz over a 150 MHz range centered at the various zero field ODMR frequencies, which lie between 1.74 and 4.25 GHz, while using an average power of ~ 75 mW.

Methods

The method employed depends critically on complete saturation of the triplet sublevels during the decay, which was confirmed by saturating two transitions simultaneously. This produces a pseudo-one-level system that provides a single exponential decay constant corresponding to the average lifetime of the triplet sublevels.

All decays were deconvoluted by a nonlinear least squares Marquardt algorithm designed to minimize the chi-square of the fitting function and whose goodness-of-fit was monitored via a residuals plot. Calculation of the set of k 's and W_{ij} 's was performed by solving the set of simultaneous equations describing the decay matrix of the saturated system (14) combined with iterative Newton-Raphson refinement. Experimental and calculated average decay constants agreed to within $\sim 10\%$ for all temperatures and solvents, providing further confirmation that the zero field transitions were saturated effectively during the measurement.

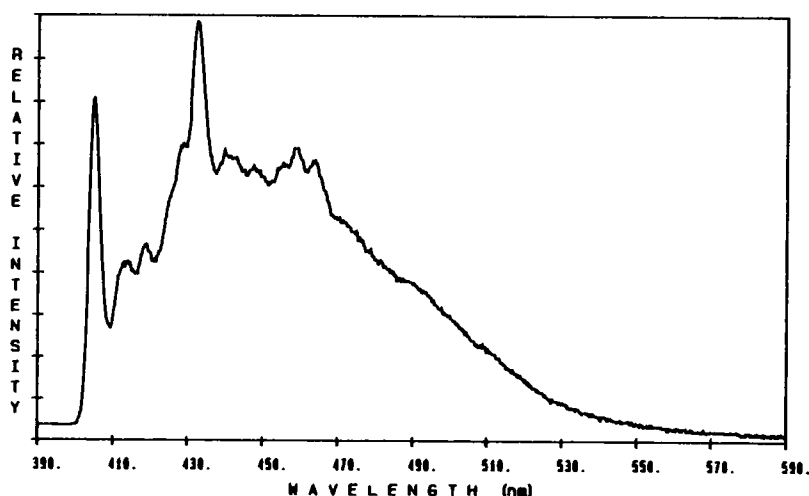


FIGURE 1 Phosphorescence emission spectrum of RNase T₁ in glycerol-phosphate buffer mixture (40% glycerol with an enzyme concentration of $\sim 1.5 \times 10^{-4}$ M) at 4.2 K, with excitation at 300 nm and emission slit resolution of 1.5 nm.

RESULTS

Phosphorescence Spectrum and Zero Field ODMR Transitions

The phosphorescence spectrum (Fig. 1) and the zero field ODMR transitions of the tryptophan residue in RNase T_1 in a glycerol and phosphate buffer (1:1 vol/vol) mixture show features similar to those observed by Hershberger et al (13) for an ethylene glycol-phosphate buffer (1:1 vol/vol) mixture. The phosphorescence shows very well resolved vibronic structure. The $|D - E|$ and $2|E|$ microwave transitions observed while monitoring the 0,0-emission band have halfwidths of ~ 50 mHz and 125 mHz, respectively. These narrow linewidths are indicative of the relatively homogeneous nature of the environment surrounding the buried tryptophan residue within the protein. Changes of the glycerol content in the glycerol-phosphate buffer medium did not affect the appearance of the phosphorescence spectra or the positions or line shapes of the ODMR transitions.

Individual SLR Rate Constants and Their Temperature Dependence

Individual SLR rate constants W_{ij} , ($i \neq j = x, y, z$) calculated for RNase T_1 in a 40% glycerol-phosphate buffer mixture are plotted as a function of temperature in Fig. 2. Spin-lattice relaxation is seen to be anisotropic and at each observed temperature within the range studied the SLR rate constants are consistently ordered $W_{yz} > W_{yx} > W_{xz}$. It is interesting to note that even at 1.2 K the W 's have significant nonzero values as observed earlier for tryptophan and tryptophan residues in other proteins (Table I).

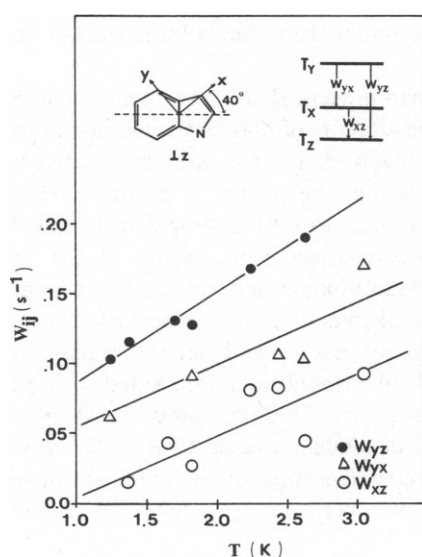


FIGURE 2 Temperature dependence of the individual SLR tryptophan rate constants. The sample is RNase T_1 at a concentration of $\sim 1.5 \times 10^{-4}$ M in a 40% glycerol-phosphate buffer mixture.

TABLE I
INDIVIDUAL SPIN-LATTICE RELAXATION RATE
CONSTANTS (s^{-1}) FOR TRYPTOPHAN AND
TRYPTOPHAN RESIDUES IN VARIOUS PROTEINS AT
LOWEST TEMPERATURES

Sample	Medium	T	W_{yz}	W_{yx}	W_{xz}	References
RNase T_1	50% GB*	1.21	0.125	0.073	0.001	This work
RNase T_1	40% GB	1.23	0.106	0.064	0.055	This work
RNase T_1	30% GB	1.51	0.157	0.182	0.047	This work
RNase T_1	20% GB	1.23	0.157	0.128	0.041	This work
Lysozyme	50% EGB†	1.30	0.084	0.0	0.006	(1)
Chymotrypsin	50% EGB	1.20	0.020	0.0	0.070	(3)
Tryptophan at pH 12	EGW§	1.34	0.138	0.117	0.146	(2)
Tryptophan at pH 7	EGW	1.30	0.036	0.0	0.036	(1)

*Glycerol in glycerol-phosphate buffer.

†Percentage ethylene glycol in ethylene glycol-phosphate buffer.

§Ethylene glycol-water (1:1 vol/vol) at selected pH.

The value of W_{yz} at any temperature in this medium, however, always is found to be less than the value of the decay constant of the most radiative sublevel (Table II) within the observed temperature range of 1.2 to 3.0 K. All the W 's within the limit of experimental scattering show an approximately linear increase as a function of temperature. This approximate linearity is observed for all solutions of differing glycerol-phosphate ratio, as well.

Effect of Medium on the Average SLR Rate Constants

The average SLR rate constants for the tryptophan residue in media having varying amounts of glycerol in the glycerol-phosphate buffer mixture (at fixed protein concentra-

TABLE II
SUBLEVEL DECAY RATE CONSTANTS (s^{-1}) FOR
TRYPTOPHAN AND TRYPTOPHAN RESIDUES IN
VARIOUS PROTEINS

Sample	Medium	k_x	k_y	k_z	References
RNase T_1	50% GB	0.256	0.100	0.054	This work
RNase T_1	40% GB	0.264	0.076	0.051	This work
RNase T_1	30% GB	0.244	0.117	0.055	This work
RNase T_1	20% GB	0.256	0.134	0.056	This work
Lysozyme	50% EGB	0.293	0.113	0.054	(1)‡
Chymotrypsin	50% EGB	0.316	0.132	0.034	(3)§
Tryptophan at pH 12	EGW	0.264	0.073	0.064	(2)
Tryptophan at pH 7	EGW	0.240	0.119	0.038	(1)

*The values refer to the average value over the entire range of temperatures mentioned in text.

‡Measured at $T = 1.3$ K.

§Measured at $T = 1.2$ K.

||Measured at $T = 1.34$ K.

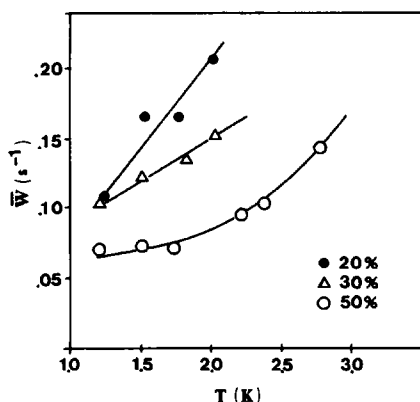


FIGURE 3 Temperature dependence of the average SLR rate constant for RNase T_1 in different media. The enzyme concentration in each solution is maintained at $\sim 1.5 \times 10^{-4}$ M. Caption represents the percentage of glycerol in the glycerol-phosphate buffer mixture.

tion) are presented as a function of temperature in Fig. 3. The results show appreciable variation in the \bar{W} with solvent composition as well as in the temperature dependence of different solutions. The temperature coefficient of \bar{W} increases quite rapidly with decreasing glycerol concentration.

In Fig. 4, \bar{W} is plotted versus glycerol concentration at 1.5 and 2.0 K. These plots show a non-linear trend and indicate that \bar{W} is more sensitive to the glycerol content of the medium at higher temperatures.

Decay Constants for Individual Sublevels

The calculated decay constants are found to be constant (to within 10%) in the temperature interval studied. In Table II the average values are presented along with those reported for lone tryptophan and tryptophan residues in other proteins.

DISCUSSION

SLR Mechanism

Spin-lattice relaxation can occur through direct, Orbach, and Raman processes (15). In the direct process the transition of a spin between states $|a\rangle$ and $|b\rangle$ is accompanied by the absorption or emission of a lattice phonon of the same energy. Using first order time-dependent perturbation theory the SLR rates (in s^{-1}) can be expressed as:

$$W = 3/2\pi(\delta_{ab}/\hbar)^3 \frac{\coth(\delta_{ab}/2kT) |\langle a|V'|b\rangle|^2}{\rho \hbar v^5} \quad (1)$$

where, $\delta_{ab} = E_b - E_a$, v = velocity of sound in the medium, and ρ = density of the medium.

The matrix element involved in the rate expression contains terms that depend only on the spin system and which are independent of the lattice temperature. The exact form of this integral and the perturbation V' depend on the spin-lattice relaxation mechanism that is operative.

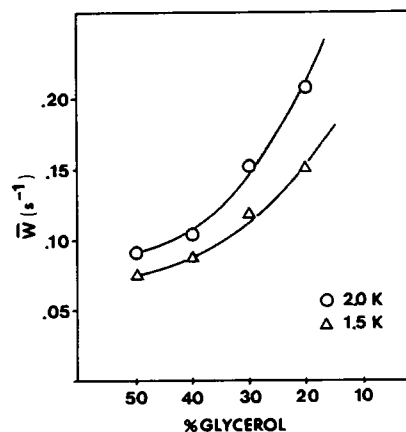


FIGURE 4 Average SLR rate constants for RNase T_1 plotted against % glycerol in the glycerol-phosphate buffer medium at fixed temperatures of 1.5 and 2.0 K.

When $\delta_{ab} \ll 2kT$,

$$\coth(\delta_{ab}/2kT) = 2kT/\delta_{ab},$$

and Eq. 1 reduces to

$$W = \frac{3 \delta_{ab}^2 kT |\langle a|V'|b\rangle|^2}{\pi \hbar^4 V^5 \rho} \quad (2)$$

The Orbach process requires that the spin transition between states $|a\rangle$ and $|b\rangle$ occurs with the participation of an upper $|c\rangle$ state. Level $|c\rangle$ is within a continuum of phonon energies, such that the transition from $|b\rangle$ to $|c\rangle$ involves absorption of a phonon having energy $(\Delta E - \delta_{ab})$, while the transition $|c\rangle$ to $|a\rangle$ results in the emission of a phonon of energy ΔE . This process is characterized by:

$$W = (\Delta E)^3 / (e^{\Delta E/kT} - 1) = (\Delta E)^3 e^{-\Delta E/kT}, \quad (3)$$

where the second relationship holds in the low temperature limit.

The Raman process also is a two phonon process, but in this instance all pairs of phonons whose energy differences are δ_{ab} are involved. In this case the excited level is not necessarily within the phonon continuum. Here two distinct mechanisms can be distinguished. The first order Raman process arises from terms in the orbit-lattice interaction Hamiltonian that are quadratic in lattice strain but are only taken to first order in perturbation theory. The second order process arises from terms that are linear in the lattice displacements and are treated with second order perturbation theory. These two processes show a T^7 and T^9 temperature dependence, respectively, when $T \ll \theta$, where θ is the Debye temperature of the medium. In the limit of $T \gg \theta$, however, both processes tends toward a T^2 dependence.

Both the Raman and Orbach relaxation mechanisms, which are second order processes, normally become insignificant within the low-temperature regime below ~ 3 K. The spin-lattice relaxation under such conditions is domi-

nated instead by some variation of the direct process mechanism involving coupling of the spin with a single lattice phonon.

A plot of $\ln W_{ij}$ vs. $1/T$ for a 40 % glycerol solution of RNase T₁ is presented in Fig. 5. Least squares linear regression was done in each case giving an apparent Orbach energy gap (ΔE) of between ~ 1 and 3 cm^{-1} depending on the particular transition. This small value for ΔE , corresponding to the spacing between the two relaxing levels and the third participating level, makes such a second-order process unlikely in this temperature range. For the case of naphthalene in durene in the fast relaxation limit, SLR was attributed to a low-lying localized phonon state, and the Orbach ΔE was found to be of the order 16 cm^{-1} . Such a level also was confirmed spectroscopically (8). In the case of aniline in *p*-xylene (10), quinoxaline in durene (16), and for zinc porphyrin in *n*-alkanes (11) the local phonon states were predicted to lie at least 20 cm^{-1} higher than the lowest triplet state.

The plot of $\ln \bar{W}$ vs. $1/T$ for a 50 % glycerol solution is presented in Fig. 6. The values of \bar{W} are consistently lower than those found in the case of a 40 % glycerol solution. The curve shows the average behavior of SLR in this solution, and no relaxation mechanism can be proposed solely in considering \bar{W} .

A log-log plot is provided in Fig. 7, showing the various $\ln W_{ij}$, ($i \neq j = x, y, z$) vs. $\ln T$ for a 40 % glycerol solution. Least squares fitting yields slopes of $\sim 0.8, 0.9$, and 1.9 for W_{yz} , W_{yx} , and W_{xz} , respectively. For both W_{yz} and W_{yx} the slopes are close to unity considering the allowance for experimental uncertainty, indicating the operation of a normal direct process. For W_{xz} , corresponding to the lowest energy transition, the slope is clearly higher than unity, although the large scatter of the data prevents an accurate estimate. This may well suggest either a phonon-limited direct process (phonon bottleneck) having a T^n (n between 1 and 2) temperature dependence, or relaxation via a

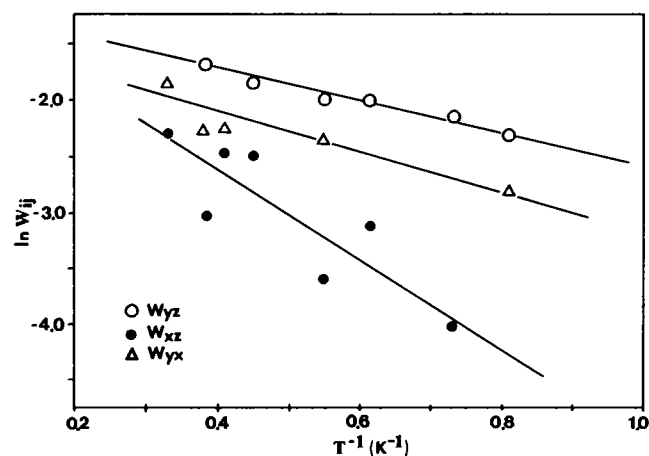


FIGURE 5 Plot of $\ln W_{ij}$ vs. $1/T$ for RNase T₁ in 40% glycerol buffer mixture with a linear least-squares line fit to data.

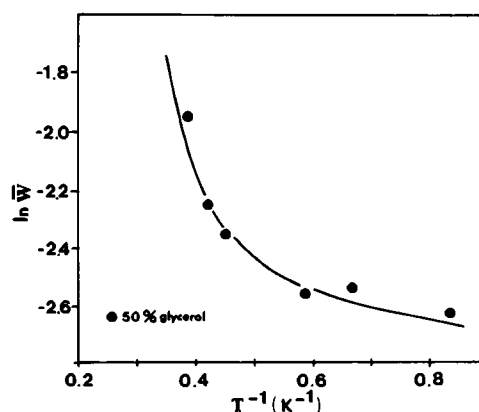


FIGURE 6 Plot of $\ln \bar{W}$ vs. $1/T$ for RNase T₁ in 50% glycerol buffer mixture.

system of two tunnelling states which would produce a T^m dependency ($m \geq 2$) (5, 17). Identification of such processes, however, requires careful analysis of SLR at temperatures at and below 1.0 K. This was not possible with the apparatus available for this present study. Evidence for these two types of direct processes has been reported by other researchers (17, and references therein). The scatter is greater in the case of W_{xz} ($\pm 17\%$) compared with W_{yx} ($\pm 7\%$) and W_{yz} ($\pm 3\%$) largely due to the low absolute value of W_{xz} . A similar trend for the temperature variation was observed for the solution containing 50 % glycerol.

Anisotropy in the Magnitude of W_{ij}

The magnitudes of the W_{ij} 's are different, with the W 's between sublevels most widely separated in energy being the largest. This pattern of anisotropy is quite different from that observed for many organic triplet states. For instance, in naphthalene in durene within the fast relaxation limit, the W between the two in-plane zero field

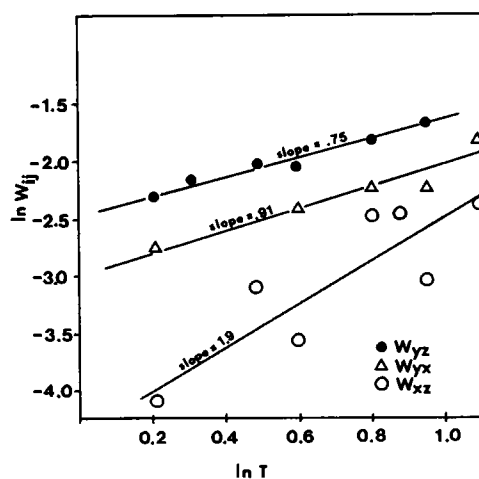


FIGURE 7 Plot of $\ln W_{ij}$ vs. $\ln T$ for RNase T₁ in 40% glycerol buffer mixture with a linear least-squares line fit to data.

sublevels is dominant. This pattern has been attributed to a special process, the rotation of the spin axes about the axis normal to the molecular plane. This occurs due to thermal promotion to a localized phonon state at ΔE of $\sim 16 \text{ cm}^{-1}$. The same pattern has been proposed in the case of zinc porphyrin in *n*-alkane (11), aniline in *p*-xylene (10), and for quinoxaline in durene (16). For naphthalene in crystalline *n*-pentane, we have found (12) that the SLR rates below 2.5 K are considerably slower than those found in a durene host and that the SLR between one of the in-plane levels and the out-of-plane level dominates, while the SLR between the in-plane sublevels is essentially zero. Hence the dominant individual sublevel SLR rate constant for this case corresponds again to the two sublevels having the largest energy separation. This pattern also has been observed in the case of acridine in biphenyl (18), triphenylene and coronene in *n*-alkane (19), and for 1, 2, 4, 5 tetrachlorobenzene in durene (20). For the present system of tryptophan within RNase T_1 , we find that the pattern of SLR is in the order $W_{yz} > W_{yx} > W_{xz}$, which is in the order of decreasing δ_{ij} . The differences may result from a difference in the density of phonon states required for relaxation processes to couple the various transitions. Although the density of phonon states in a regular three-dimensional crystalline solid is proportional to δ_{ab}^2 , the W_{ij} are not similarly proportional to δ_{ij}^2 . It is not reasonable to expect that the density of phonon states in our enzyme-glassy solvent matrix follows the same dependence on δ_{ab} as it does in a crystalline solid. Our results show that the W_{ij} increases less rapidly with energy than δ_{ij}^2 , implying that the phonon density of states increases more slowly than δ_{ab}^2 . This is consistent with the fractal theory of Stapelton (5) where the density of states is known to vary as $\delta_{ab}^{(d-1)}$, where d is the fractal dimensionality of the system.

The interpretation of SLR in terms of the phonon density of states in our system is complicated further by the apparent phonon bottleneck which appears in the lowest energy relaxation process. A phonon bottleneck would appear as an anomalously low density of phonon states at the corresponding frequency. From the data in Fig. 2, however, we find that $W_{yz}/W_{yx} = 1.7$ over the temperature range investigated. Since SLR between these sublevels apparently is due to a nonbottleneck direct process (Fig. 7), and since $\delta_{yz}/\delta_{yx} = 1.7$, the implication is that the density of phonon states available to tryptophan in the enzyme is more nearly linear with frequency than quadratic. This analysis implicitly assumes that the coupling of the spins with the lattice phonons is isotropic so that W varies only with the density of phonon states and does not depend on the particular spin transition that occurs. This may not be the case, so the analysis should be treated with appropriate caution.

Effect of Medium

It has been found that the host has a very significant effect on the SLR rate constants. In the case of pyrazine (21)

where the SLR rate constants in the range of 2 to 8 K were best explained as the sum of a direct and a Raman process, it has been observed that SLR is strongly sensitive to the choice of solvent. Even for the same solvent, subtle differences in the lattice structure induced by different rates of sample cooling were sufficient to produce measurable changes in the SLR rate constants. This has been explained in terms of the involvement of anharmonic Raman processes, which are known to depend strongly on the physical state of the host lattice structure. In the case of the naphthalene triplet state, the host has been found to have a pronounced effect on SLR rate constants, including the pattern of anisotropy of the individual SLR rates (8, 12, 22). For zinc porphyrin in an *n*-alkane polycrystalline matrix it has also been observed that changing of the *n*-alkane chain length affects the SLR rate quite remarkably (11). In this study (11) an Orbach process has been proposed, while differences observed in various *n*-alkane solvents have been attributed to a solvent dependence of the ΔE for the localized phonon state.

For paramagnetic iron proteins (5, 17 and references therein), the environment has been found to affect the electron SLR. The low temperature relaxation rate in cytochrome *c* switches from a T^1 to a T^2 dependence when the protein environment is changed from a frozen solution to a freeze-dried sample, while the Raman relaxation rate at higher temperature remains unaffected. Changes in the host lattice induced by a change in the ionic strength of the medium also affect the temperature dependence in some instances (17).

SLR rate constant data have been reported (1-3) for the triplet state of tryptophan and of the tryptophan residue in several enzymes at temperatures near 1.2 K. In the case of tryptophan, the pH of the medium apparently has an influence on the SLR rate constants (1, 2). Results presented in this work for RNase T_1 show an appreciable dependence of SLR on the percentage of glycerol present in the medium. These results are consistent with our earlier unpublished observations that the S/N (signal-to-noise) ratio of tryptophan slow passage ODMR spectra decreases as solutions of lower glycerol concentration are used.

Tryptophan Sublevel Decay Constants

Sublevel decay constants given in Table II are comparable to those found in the case of free tryptophan and for tryptophan residues in other atypical enzymes. The decay rate constants for tryptophan subject to different environments are all within about $\pm 20\%$ of the average value, which tends to indicate that the environment has very little effect on the total decay constants. The zero field splitting, and phosphorescence Stoke's shifts are quite sensitive to changes in the local tryptophan environment, however.

CONCLUSION

The individual and average spin-lattice relaxation (SLR) rate constants in the low relaxation limit for the triplet

state of the lone tryptophan residue in RNase T_1 have been discussed in terms of mechanisms known to be possible within the temperature regime studied. The solvent environment of the protein has been found to have a most definite effect on the SLR rate constants which, however, is not reflected in the optical spectrum or in the zero field ODMR transitions.

Within the temperature range investigated ($1.2 \rightarrow 3.0$ K), the individual SLR rate constants are approximately linear with temperature for the dominant relaxation processes W_{yz} and W_{yx} . On the other hand, the slower relaxation, W_{xz} , appears to vary approximately as T^2 (Fig. 7). However, further study around 1 K would be required to confirm a quadratic dependence on T , which is suggestive of a phonon-bottlenecked process for the $T_x \leftrightarrow T_z$ relaxation pathway.

Of further interest is the dependence of SLR on the solvent composition. Although the tryptophan residue of RNase T_1 is known to be buried in the interior of the enzyme (13, 23–26), the SLR of its triplet state is observed to become more efficient as the glycerol content of the cryosolvent is reduced (Fig. 3, 4). On the other hand, other properties of the T_1 state, such as the phosphorescence spectrum, the individual sublevel decay constants (Table II), and the ZFS frequencies are found to be independent of the cryosolvent composition. This feature suggests that there is little effect of the cryosolvent composition on the enzyme conformation in the vicinity of the tryptophan residue. Some features associated with the solvent composition do influence the SLR, however, in an indirect manner. It appears, for instance, that the atoms of the enzyme structure are coupled strongly to those of the solvent so that the tryptophan residue is influenced by the solvent phonon structure. Variability in solvent composition could be associated either with changes in the phonon density of states of the solvent, with the coupling between enzyme and solvent atoms, or with both. Whatever the mechanism, SLR increases as the glycerol content of the solvent is reduced. From a practical point of view, tryptophan ODMR signals of proteins are expected to become weaker at low glycerol concentrations, since enhanced SLR leads to smaller steady-state spin alignments, which are a requirement for ODMR. This is consistent with our previous unpublished experience that ODMR signals of tryptophan in enzymes cannot be observed when the ethylene glycol content of this aqueous solvent is reduced below a certain limit. This disappearance of ODMR signals occurs for both tryptophan residues, which are on the protein surface and therefore directly exposed to the solvent, as well as for buried residues, confirming the fact that the latter are in close communication with the solvent medium.

This work was supported by U.S. National Science Foundation grant NSF-CHE 82-07265.

Received for publication 10 May 1985 and in final form 23 September 1985.

REFERENCES

1. Zuchlich, J., J. U. von Schütz, and A. H. Maki. 1974. Direct measurement of spin-lattice relaxation rates between triplet spin sublevels using optical detection of magnetic resonance. *Mol. Phys.* 28:33–47.
2. Rouslang, K. W., and A. L. Kwiram. 1976. Triplet state decay and spin-lattice relaxation rate constants in tryrosinate and tryptophan. *Chem. Phys. Lett.* 39:226–230.
3. Maki, A. H., and T. T. Co. 1976. Study of triplet-singlet energy transfer in an enzyme-dye complex using optical detection of magnetic resonance. *Biochemistry*. 15:1229–1235.
4. Stapleton, H. J., J. P. Allen, C. P. Flynn, D. G. Stinson, and S. R. Kurtz. 1980. Fractal form of proteins. *Phys. Rev. Lett.* 45:1456–1459.
5. Allen, J. P., J. T. Colvin, D. G. Stinson, C. P. Flynn, and H. J. Stapleton. 1982. Protein conformation from electron spin relaxation data. *Biophys. J.* 38:229–310.
6. Wolfe, J. P. 1971. Direct measurement of spin-lattice relaxation rates for the localized triplet state in molecular crystals; evidence for one-and two-phonon process. *Chem. Phys. Lett.* 10:212–218.
7. Fischer, P. H. H., and A. B. Dennison. 1969. Anisotropic saturation of the electron spin resonance in the photo-excited triplet state of pyrene- d_{10} . *Mol. Phys.* 17:297–304.
8. Verbeek, P. J. F., H. J. den Blanken, and J. Schmidt. 1979. The anisotropy of the spin-lattice relaxation in the lowest triplet state of naphthalene in durene in the presence of a magnetic field. *Chem. Phys. Lett.* 60:358–363.
9. Orbach, R. 1961. Spin-lattice relaxation in rare-earth salts: field dependence of the two phonon process. *Proc. Roy. Soc. Lond. A.* 264:458–495.
10. van Noort, H. M., C. A. van't Hof, B. Wirtzner, and J. Schmidt. 1981. The phosphorescent triplet state of aniline in a *p*-xylene host crystal: a study of spin-spin and spin-lattice relaxation. *Chem. Phys. Lett.* 81:351–356.
11. van Noort, H. M., B. Wirtzner, J. Schmidt, and J. H. van der Waals. 1982. The phosphorescent 3E_u state of zinc porphyrin in *n*-alkane host crystals. Temperature dependence of the electron spin resonance transition and spin-lattice relaxation in zero-field. *Mol. Phys.* 45:1259–1269.
12. Ghosh, S., J. W. Weers, M. Petrin, and A. H. Maki. 1984. Anisotropic spin-lattice relaxation in the triplet state of naphthalene- h_8 in *n*-pentane. *Chem. Phys. Lett.* 108:87–92.
13. Hershberger, M. H., A. H. Maki, and W. C. Galley. 1984. Phosphorescence and optically detected magnetic resonance studies of a class of anomalous tryptophan residues in globular proteins. *Biochemistry*. 19:2204–2209.
14. Co, T., R. J. Hoover, and A. H. Maki. 1974. Dynamics of the tyrosine triplet state from magnetic resonance-saturated phosphorescence decay measurements. *Chem. Phys. Lett.* 27:5–9.
15. Standley, K. J., and R. A. Vaughan. 1969. *Electron Spin Relaxation Mechanisms in Solids*. Plenum Publishing Corp., New York. 1–74.
16. van Noort, H. M., B. Wirtzner, and J. Schmidt. 1982. Determination of the individual spin-lattice relaxation rates between the spin levels of phosphorescent triplet-state molecules. *Chem. Phys. Lett.* 85:359–364.
17. Muench, P. J., T. R. Askew, J. T. Colvin, and H. J. Stapleton. 1984. Electron spin relaxation in myoglobin below 1 K: positive identification of a phonon bottleneck. *J. Chem. Phys.* 81:63–65.
18. Anthunis, D. A., B. J. Botter, J. Schmidt, P. J. F. Verbeek, and J. H. van der Waals. 1975. Spin-lattice relaxation in the phosphorescent triplet state of acridine and phenanthrene in zero magnetic field. *Chem. Phys. Lett.* 36:225–228.
19. Nishi, N., K. Matsui, M. Kinoshita, and J. Higuchi. 1979. Study on the triplet state of triphenylene by microwave induced delayed phosphorescence and $T \leftarrow S$ excitation spectroscopy. *Mol. Physics*. 38:1–24.

20. Lutz, D. R., K. A. Nelson, R. W. Olson, and M. D. Fayer. 1978. Spin-lattice relaxation in triplet states of isolated molecules and pure crystals in zero field. *J. Chem. Phys.* 69:4319-4312.
21. Hall, L. H., and M. A. El-Sayed. 1975. Temperature dependence of the spin-lattice relaxation rates in the triplet state of pyrazine at low temperature. *Chem. Phys.* 8:272-288.
22. Schwoerer, M., U. Konzelman, and D. Kilpper. 1972. Spin-phonon interaction for triplet state molecules in organic mixed crystals. *Chem. Phys. Lett.* 13:272-277.
23. Longworth, J. W. 1968. Excited state interactions in macromolecules. *Photochem. Photobiol.* 7:587-596.
24. Eisinger, J., and G. Navon. 1969. Fluorescence quenching and isotope effect of tryptophan. *J. Chem. Phys.* 50:2069-2077.
25. Eftink, M. R., and C. A. Ghiron. 1975. Dynamics of a protein matrix revealed by fluorescence quenching. *Proc. Natl. Acad. Sci. USA.* 72:3290-3294.
26. Imakubo, K., and Y. Kai. 1977. Phosphorescence of ribonuclease T₁ in solution at 293 K. *J. Phys. Soc. Jpn.* 42:1431-1432.